



Estimation of Fractures Orientation from qP wave of Multiazimuthal AVO

Ellen N.S.Gomes^{*1)}, Jessé C. Costa¹⁾, João dos S. Protázio²⁾ and Ivan A. Simões Filho³⁾, ¹⁾CPGf / UFFa, ²⁾ Dep. Matemática / UFFa and ³⁾PUC/RJ.

Copyright 2003, SBGF - Sociedade Brasileira de Geofísica

This paper was prepared for presentation at the 8th International Congress of The Brazilian Geophysical Society held in Rio de Janeiro, Brazil, 14-18 September 2003.

Contents of this paper was reviewed by The Technical Committee of The 8th International Congress of The Brazilian Geophysical Society and does not necessarily represents any position of the SBGF, its officers or members. Electronic reproduction, or storage of any part of this paper for commercial purposes without the written consent of The Brazilian Geophysical Society is prohibited.

Abstract

We investigate the estimation of fractures orientation, strike and dip, through multiazimuthal AVO analysis of qP and its converted waves. We assume weak impedance contrast, weak anisotropy and that the fractured medium behaves as an effective transversally isotropic (TI) medium. Under these assumptions fractures orientation is reduced to the estimation of the axis of symmetry of the TI medium from qP reflectivity data. Linearized approximations of qP reflectivity are used for inversion. SVD analysis and numerical simulations show that qP, qS₁ and qS₂ are required to produce stable estimates of fractures orientation. Although the inversion produces unstable results for some contrasts of elastic parameters the subset of parameters necessary to recover the TI symmetry axis can be recovered stably from AVO/AVD data.

Introduction

Most hydrocarbon reservoirs occur in fractured formations. In this case, fractures mainly control the reservoir permeability. Since wave propagation in fractured media might be modeled through an effective anisotropic medium (Hudson, 1982, Schoenberg and Sayers, 1995), the characterization of the reservoir elastic anisotropy from seismic data may help optimizing oil recovery. Previous works report fractures characterization from AVO/AVD data. Rüger and Tsvankin (1995, 1997) show how to estimate vertical fractures strike and fluid content information from qP reflection coefficients data. Pérez et al. (1999) use shear wave splitting and P wave reflection data to determine the strike of a vertical set of fractures. Beretta et al. (2002) use diffraction tomography to estimate the fractures density also for vertically fractured medium. We formulate the problem of fractures characterization using the reflections coefficients of a qP incident wave, including converted waves. The incidence medium is isotropic and we assume weak impedance contrast and weak anisotropy. Linearized expressions for qP reflectivity (R_{qPqP} , R_{qS1qP} , R_{qS2qP}) (Gomes et al., 2001) are used for inversion. The fractured media is considered as an effective TI medium. The problem of determining fractures orientation is posed as the estimation of the axis of symmetry of this medium from qP reflectivity.

The linearized qP reflectivity across an interface separating two weak impedance contrast and weak anisotropic media was presented by Gomes et al. (2001). The two anisotropic media are considered as small

perturbations around an isotropic homogeneous background. Along the sagittal plane the expressions are:

$$R_{qPqP} = \frac{1}{2\rho\alpha^2} \left\{ \Delta C_{11} \tan^2 \theta \sin^2 \theta + 2 [\Delta(C_{13} + 2C_{55}) - 4\Delta C_{55}] \sin^2 \theta + \Delta C_{33} \cos^2 \theta \right\} + \left(1 - \frac{1}{2 \cos^2 \theta} \right) \frac{\Delta\rho}{\rho} \quad (1)$$

$$R_{qS1qP} = \frac{1}{2\rho\alpha^2\eta(\theta)} \left\{ 2\Delta C_{11} \sin^2 \theta + [2\Delta(C_{13} + 2C_{55}) - 4\Delta C_{55}] \sin \theta \cos 2\theta - \Delta C_{33} \sin 2\theta \cos \theta + \frac{1}{\kappa K(\theta)} \left\{ 2\Delta C_{15} \sin^2 \theta (2\kappa\omega(\theta) - 1) + 2\Delta C_{35} \cos \theta (\cos \theta - 2K(\theta)\omega(\theta)) + 2\Delta C_{55} \sin 2\theta (\kappa^2 \sin^2 \theta - K^2(\theta)) \right\} \right\} - \left(\frac{\sin \theta}{K(\theta)} \right) \frac{\Delta\rho}{\rho} \quad (2)$$

$$R_{qS2qP} = \frac{1}{\rho\alpha^2 K(\theta)} \left\{ \frac{1}{\kappa} \left\{ \Delta C_{14} \sin^2 \theta + \Delta C_{45} \sin 2\theta + \Delta C_{34} \cos^2 \theta \right\} - \frac{1}{\eta(\theta)} \left\{ \Delta C_{16} \sin^3 \theta + \Delta(C_{14} + 2C_{55}) \cos \theta \sin^2 \theta + \Delta(C_{36} + 2C_{45}) \cos^3 \theta \sin \theta + \Delta C_{34} \cos^2 \theta \right\} \right\} \quad (3)$$

Where θ is the incidence angle; $\kappa = \beta/\alpha$ is the ratio between S-wave and P-wave velocities in the background, ρ is the background density; $\Delta\rho$ is the average density contrast across the interface and ΔC_{ij} is the average elastic parameters contrast between the two media; $K(\theta) = \sqrt{1 - \kappa^2 \sin^2 \theta}$, $\omega(\theta) = \kappa \sin^2 \theta + K(\theta) \cos \theta$ and $\eta(\theta) = \kappa \cos \theta + K(\theta)$. Equations (1) was presented previously by Vavryčuk & Pščenčík (1998) and (2) and (3) where also derived in Jílek (2002) in a somewhat different form. In order to derive the expression above, the polarization directions in the background media were chosen to be the SV and SH direction, which makes them more suitable when the medium of incidence has azimuthal symmetry. We assume that the medium of incidence is isotropic and coincides with the background media used for linearization. In this case, $\Delta C_{ij} = (C_{ij}^T - C_{ij}^0) / 2$, where C_{ij}^T indicates the transmission medium elastic tensor and C_{ij}^0 is the background elastic tensor.

Estimation of Fractures Orientation

In order to estimate the fractures orientation we make the following assumptions:

1- The fractured medium behaves as an effective TI medium with its axis of symmetry perpendicular to the plane of fractures.

2- The incidence medium is isotropic.

Under these assumptions, our goal is to estimate the orientation of the symmetry axis from the elastic parameters estimated from inversion. If the axis of symmetry is not aligned with one of the coordinate axis the plane of symmetry containing the axis forms an angle Ψ with the x_2 (Figure 1). This angle can be determined from the relation:

$$\tan 2 \Psi = \frac{2(C_{16} + C_{26})}{C_{22} - C_{11}} \quad (4)$$

Unfortunately four angles have the same tangent Ψ , $\Psi+\pi/2$, $\Psi-\pi/2$, $\Psi+\pi$. Rotating the elastic parameters estimated by the negative of one of these angles aligns the symmetry plane containing the tilted axis along the x_1 or x_2 axis. We can always choose the rotation, which align the symmetry plane containing the tilted axis along x_2 axis and use the expression below to determine the dip angle Θ

$$\tan 2 \Theta = \frac{2(C_{15} + C_{35})}{C_{33} - C_{11}} \quad (5)$$

Under our assumptions, dip angle can be estimated from the inversion results except by the same ambiguity as before, i.e., Θ or $\Theta+\pi/2$. This ambiguity can be resolved rotating the parameter by the negative of Θ and observing the differences $C_{11}-C_{22}$ and $C_{33}-C_{22}$. If the first difference is zero the axis of symmetry is aligned along x_3 and the dip angle is $\Theta+\pi/2$ otherwise $C_{33}-C_{22}$ is zero and the axis is aligned along x_2 and the dip angle is Θ . It is always possible to perform this rotation, all the combination of elastic parameters required to perform this rotation are estimated from inversion.

If the axis of symmetry coincides with one of the coordinate axis the algorithm fails. In this case orientation can be determined using the alternatives:

- If $C_{22}=C_{33}$ and $C_{44} \neq C_{55}$ the axis is along x_1 ;
- If $C_{11}=C_{33}$ and $C_{44} \neq C_{55}$ the axis is along x_2 ;
- If $C_{11}=C_{22}$ and $C_{44} = C_{55}$ the axis is along x_3 .

The next step investigates if this algorithm is stable. Using the equation (1)-(3) the inversion problem is reduced to the solution of a linear system

$$\mathbf{r} = \mathbf{A}(\mathbf{C}^0, \Psi, \Theta) \mathbf{p}, \quad (7)$$

Where \mathbf{r} is the vector containing the observations (R_{qPqP} , R_{qS1qP} , R_{qS2qP}), \mathbf{p} is the vector containing the density and elastic parameters contrasts and the matrix $\mathbf{A}(\mathbf{C}^0, \Psi, \Theta)$ depends only on the background medium and the direction of the incident P wave. SVD analysis of \mathbf{A} shows that it is required at least six azimuths equally spaced, 30° interval, and incident angles greater than 15° to produce stable estimates. Multi-azimuthal walkway experiments (Leaney et al., 1999) might provide this kind of data.

The vector \mathbf{p} is organized as bellow:

$$\begin{aligned} p_1 &= \Delta C_{11} & p_2 &= \Delta(C_{12} + 2C_{66}) & p_3 &= \Delta(C_{13} + 2C_{55}) \\ p_4 &= \Delta C_{22} & p_5 &= \Delta(C_{23} + 2C_{44}) & p_6 &= \Delta C_{33} \\ p_7 &= \Delta C_{44} & p_8 &= \Delta C_{55} & p_9 &= \Delta C_{14} \\ p_{10} &= \Delta C_{15} & p_{11} &= \Delta C_{16} & p_{12} &= \Delta C_{24} \\ p_{13} &= \Delta C_{25} & p_{14} &= \Delta C_{26} & p_{15} &= \Delta C_{34} \\ p_{16} &= \Delta C_{35} & p_{17} &= \Delta C_{36} & p_{18} &= \Delta C_{45} \\ p_{19} &= \Delta C_{46} & p_{20} &= \Delta C_{56} & p_{21} &= \Delta \rho / \rho \end{aligned} \quad (8)$$

The resolution and stability of the inversion was evaluated using SVD and numerical simulations. For the simulations several synthetic data sets were computed using the exact expressions for the reflection coefficients. Each synthetic data set was contaminated by Gaussian noise using 100 random seeds to initialize the random number generator. These data were inverted and the mean and standard deviations of the parameters used to evaluate stability

Examples

The orientation the axis symmetry was estimated the of inversion from (1), (2) and (3) joins for two models. The synthetic data set was generated solving the Zoeppritz equations (Gomes, 1999). The azimuth range is from 0° to 360° with 15° intervals and the incidence angle varies from 0° to 30° with 1° intervals. This data set was contaminated with different level Gaussian random noise of amplitude of 5% to 20% of the mean absolute value of the observations. The 100 data sets, each with a different noise contamination, were inverted. Both models have weak contrast $\Delta \rho / \rho$, $\Delta \alpha / \alpha$, $\Delta \beta / \beta$ are smaller than 0.1 and weak anisotropy.

In the first model the top medium is an isotropic $\rho = 2.65 \text{g/cm}^3$, $\alpha = 4.00 \text{km/s}$, $\beta = 2.31 \text{km/s}$. The bottom medium is TI with horizontal axis and its density is $\rho = 2.5 \text{g/cm}^3$ and its elastic tensor is:

$$C_{ij} = \begin{bmatrix} 31.26 & 13.61 & 3.34 & 0.00 & 0.00 & 0.00 \\ & 31.26 & 3.34 & 0.00 & 0.00 & 0.00 \\ & & 22.49 & 0.00 & 0.00 & 0.00 \\ & & & 6.49 & 0.00 & 0.00 \\ & & & & 6.49 & 0.00 \\ & & & & & 8.82 \end{bmatrix} \quad (9)$$

In this model (4) and (5) fails because the symmetry axis of the bottom medium coincides with the coordinate axis x_1 . We must use (6) in order to estimate the orientation of the symmetry axis. The numerical simulations results for this model with 10% noise level are in Table 1, which presents the average of the estimates of p_1 to p_8 and the ratio of the standard deviation of the estimation over its average value. The difference between C_{22} and C_{33} is smaller than the difference between these parameter and C_{11} . Noticing also the difference between C_{44} and p_8 C_{55} , we conclude the medium is TI with horizontal axis. The results are same for 20% noise level.

In the second model the top medium is isotropic $\rho = 2.60 \text{g/cm}^3$, $\alpha = 4.600 \text{km/s}$ and $\beta = 2.810 \text{km/s}$. The bottom medium is a sandstone, its elastic tensor is TI with vertical axis and its Thomsen parameters (Thomsen, 1986) are ρ

$= 2.50\text{g/cm}^3$, $\alpha = 4.476\text{km/s}$ and $\beta = 2.841\text{km/s}$, $\varepsilon = 0.097$, $\delta = 0.091$, $\gamma = 0.051$. This medium was rotated of 60° anticlockwise around x_3 axis and after that rotated of 30° clockwise around the new x_2 axis (see Figure 1). Figures 2-4 present the stereogram of the exact synthetic data for each wave type. Figures 5-7 present the corresponding stereogram computed from the mean of the parameters estimated from 100 numerical simulations. The symmetry of the R_{PP} stereogram indicates its insensitivity to the dip of fractures. However, the SVD shows that R_{PP} data is required to estimate the fractures dip. The estimated models fit the data with maximum residual of the order of 10^{-3} for every data set. The SVD analysis and the standard deviation of the parameters in the numerical simulation show that although parameters C_{14} , C_{15} , C_{16} , C_{24} , C_{25} , C_{26} , C_{36} , C_{45} , C_{46} , C_{56} present instability, but the estimative of the symmetry axis orientation is stable. The results of the numerical simulations for this model for several noise levels are presented in Table 2, which presents the average of the estimates of the symmetry axis azimuth and dip and the ratio of the standard deviation of the estimation over their average value.

Results

Several tests were performed with models with weak impedance contrast and weak anisotropy and also with models that violated some of these assumptions. Also different azimuth ranges and incidence angles were used. From these test we drew the following:

- 1- R_{qPqP} , R_{qS1qP} and R_{qS2qP} are required to recover the orientation from multiazimuthal AVO data only.
- 2-The minimum azimuth interval to recover stable estimates of orientations is $\Psi = 30^\circ$.
- 3- The minimum incidence angle range is $\Theta = 30^\circ$.
- 4- Though the estimates of elastic parameters contrasts vary during the simulations, the estimates of the orientation angles are reliable for moderate noise levels ($<10\%$).
- 5- The estimates of fractures strike is more sensitive to noise than the fractures dip.
- 6- The estimates are accurate only for models with weak impedance contrast and weak anisotropy.

Conclusions

We presented an algorithm to estimate fractures orientation from multiazimuthal AVO analysis. In order to estimate the fractures orientation AVO data only we need R_{PP} , R_{qS1qP} and R_{qS2qP} data. Though the assumption of an effective TI behavior for fractures is restrictive, its validity can be checked from the symmetries of the elastic tensor derived from the parameters inverted. For a weak anisotropic medium and weak impedance contrast, the estimates of fractures orientation are unique, except for a

90° rotation of the dip angle and, stable for moderate noise levels.

Acknowledgments

The authors acknowledge the financial support of the Project FINEP/CTPETRO/UFFPA.

References

- Beretta, M. M., Bernasconi, G. and Drufuca, G., 2002.** AVO and AVA Inversion of Fractured Reservoir Characterization. *Geophysics*, 67(1), 300-306.
- Hudson, J. A., 1982.** Wave speeds and attenuation of elastic waves in material containing cracks. *Geophys. J. R. astr. Soc.*, 64, 133-150.
- Gomes, E., 1999.** Reflectivity of P waves in anisotropic media (in Portuguese). Master Thesis. Department of Mathematics of Universidade Federal do Pará, Brazil.
- Gomes, E., Protázio, J.S, Costa, J. Simões-Filho, I.A.** 2001. Linearization of qP wave reflection coefficients in anisotropic media (in Portuguese). *Brazilian Journal of Geophysics*. 19, 48-60.
- Jilek, P., 2002,** Converted PS-wave reflection coefficients in weakly anisotropic media. *Pure and Applied Geophysics*, 7-8, 1527-1562.
- Leaney, W. S, Sayers, C. M. and Miller, D. E., 1999,** Analysis of multiazimuthal VSP data for anisotropy and AVO: *Geophysics*, 64(4), 1172-1180
- Perez, M. A., Gibson, R. L. and Toksoz, N., 1999** Detection of Fracture Orientation Using Azimuthal Variation of P-wave AVO Responses. *Geophysics*, Soc. Of Expl. Geophys., 64, 1253-1265.
- Rüger, A. and Tsvankin, I., 1995,** Azimuthal variation of AVO response for fractured reservoir. 65th Ann. Internat. Mtg., Soc. Expl. Geophys. Expanded Abstract, 1103-1106.
- Rüger, A. and Tsvankin, I., 1997,** Another Perspective on AVO crossplotting. *The Lead Edge*, 16(9), 1233-1237.
- Schoenberg, M. & Sayers, C. M., 1995.** Seismic Anisotropy of Fractures. *Geophysics*, Soc. of Expl. Geophys., 60, 204-211.
- Vavryčuk, V. & Pšenčík, V., 1998.** PP-Wave reflection coefficients in weakly anisotropic elastic media. *Geophysics*, 63(6), 2129-2141.
- Thomsen, L., 1986.** Weak elastic anisotropy. *Geophysics*, 51(10), 1954-1966.

Tabel 1 - Exact value, estimated value and standard deviation to elastic parameters. The noise level is 10%.

Elastic parameter	Extac value	Estimated Value	Standard Deviation
C_{11}	31.10	31.93	0.65%
$C_{12}+2C_{66}$	35.13	35.60	0.5%
$C_{13}+2C_{55}$	35.13	34.55	0.74%
C_{22}	40.43	40.73	0.54%
$C_{23}+2C_{44}$	40.41	39.71	0.65%
C_{33}	40.43	39.90	0.07%
C_{44}	13.86	13.69	0.35%
C_{55}	12.38	12.17	0.39%

Table 2 - Numerical simulation results for different noise levels. The ratio of the standard deviation of the estimates over the average value is also presented to indicate the stability.

Noise Level	Fract. Azimuth (Exact value $\Psi = 60^{\circ}$)	Variation	Fract. Dip (Exact value $\Theta = 30^{\circ}$)	Variation
5%	59.53°	$\pm 5^{\circ}$	25.50°	$\pm 2^{\circ}$
10%	59.95°	$\pm 10^{\circ}$	25.35°	$\pm 4.3^{\circ}$
20%	41.17°	$>40^{\circ}$	18.9°	$\pm 12.6^{\circ}$

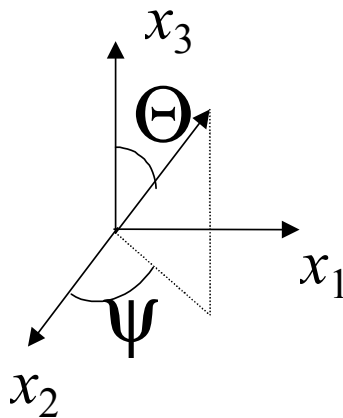
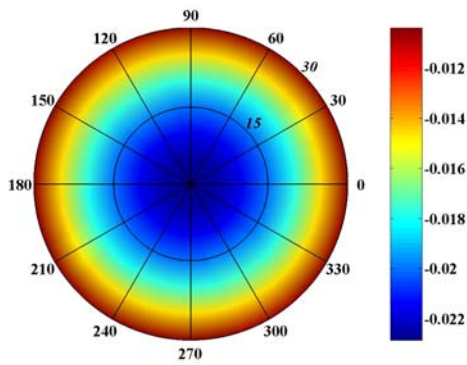
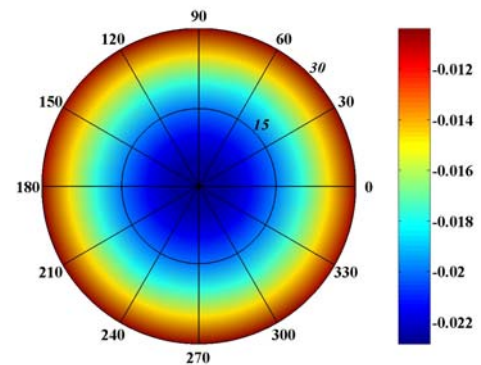
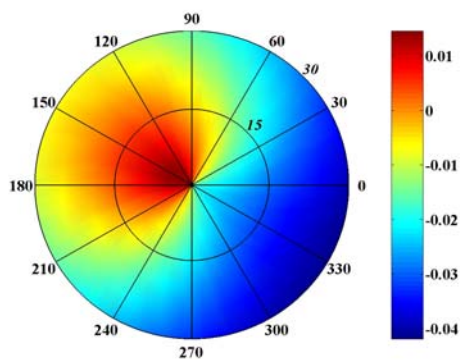
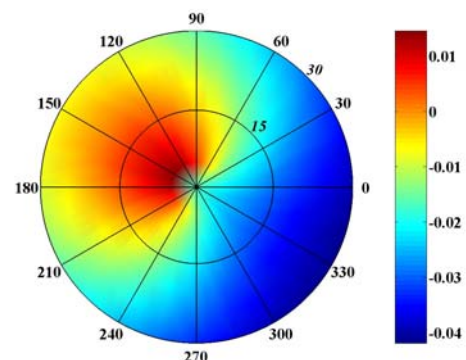
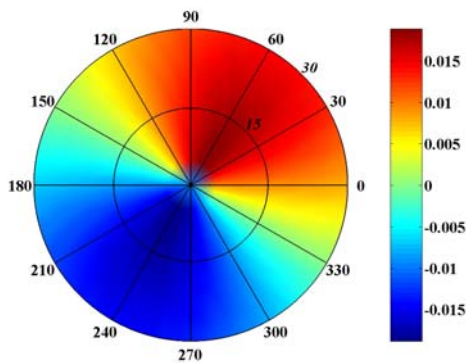
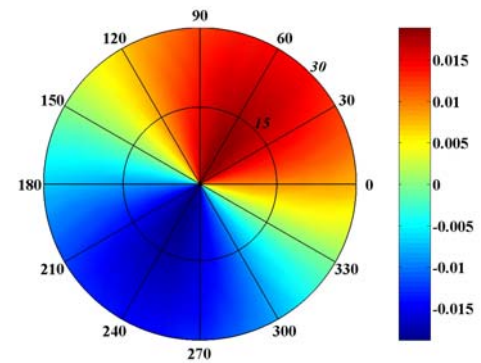


Figure 1 - Coordinate axis. The angle Ψ is the azimuthal and the angle Θ is the incidence.

Figure 2 – Stereogram for the exact $R_{qP}qP$.Figure 5 – Stereogram for the $R_{qP}qP$ of the inverted model.Figure 3 - Stereogram for the $R_{qS1}qP$ of the inverted model.Figure 6 – Stereogram for the exact $R_{qS1}qP$.Figure 4 – Stereogram for the exact $R_{qS2}qP$.Figure 7 – Stereogram for the $R_{qS2}qP$ of the inverted model.